

In silico Screening of Monoamine Oxidase B Inhibitors for the Treatment of Central Nervous System Disorders

Anderson L. P. da Costa,^{1b} Henrique B. Lima,^c Ana C. J. Silva,^{a,b} Gabrieli S. Oliveira,^{a,d} Mariana P. Barcelos,^e Carlos H. T. P. da Silva^e and Lorane I. S. Hage-Melim^{1b}*,^{a,b,d}

^aLaboratório de Química Farmacêutica e Medicinal (PharMedChem), Universidade Federal do Amapá, Rodovia Josmar Chaves Pinto, km 02, Jardim Marco Zero, 68903-419 Macapá-AP, Brazil

^bPrograma de Pós-Graduação em Inovação Farmacêutica, Rodovia Josmar Chaves Pinto, km 02, Jardim Marco Zero, 68903-419 Macapá-AP, Brazil

^cPrograma de Pós-Graduação em Ciências Farmacêuticas (PPGCF), Universidade Federal do Rio Grande do Sul (UFRGS), 90610-000 Porto Alegre-RS, Brazil

^dDepartamento de Ciências Biológicas e da Saúde, Universidade Federal do Amapá, Faculdade de Farmácia, Rodovia Josmar Chaves Pinto, km 02, Jardim Marco Zero, 68903-419 Macapá-AP, Brazil

^ePrograma de Pós-Graduação em Biociências e Biotecnologia, Faculdade de Ciências Farmacêuticas de Ribeirão Preto, Universidade de São Paulo, 14040-900 Ribeirão Preto-SP, Brazil

Worldwide, millions of people suffer from neurological and psychiatric conditions, such as schizophrenia, depression, and neurodegenerative diseases. These conditions are often linked to hyperactivity of monoamine oxidase B (MAO-B) in the brain, and inhibiting this enzyme can reduce oxidative stress, stabilize neurotransmitter levels, and alleviate symptoms. In this context, a pharmacophoric model was created using PharmaGist with 31 hits extracted from BindingDB to enable a pharmacophoric-based search of potential MAO-B inhibitors in ZincPharmer's chemical space, followed by the building of 10 conformers for each molecule in the software OMEGA, screening for structural and electrostatic similarity to safinamide using ROCS (Rapid overlay of chemical structures) and EON (Electrostatic similarity for lead-hopping), respectively. In addition, the molecular docking with Gold using the score function was performed to rank the ligands with the highest probabilities of affinity to MAO-B and then discriminate those with suitable physical-chemical, pharmacokinetic, and toxicological features using the tools QikProp, SwissADME, and DEREK. Four potential ligands with selective MAO-B inhibitor properties were identified, which show promise as future therapeutic agents for MAO-B-related disorders.

Keywords: enzyme inhibitors, monoamine oxidase B, central nervous system, *in silico*

Introduction

Enzymes known as monoamine oxidases are members of the flavoprotein oxidase family. They catalyze the reduction of the flavin adenine dinucleotide (FAD) cofactor, which oxidizes primary and secondary amines. Subsequently, the substrate is hydrolyzed non-enzymatically, releasing ammonia and forming a functional group aldehyde through water condensation. The cofactor is then regenerated by

oxidizing it with molecular oxygen, producing hydrogen peroxide as a reaction byproduct.¹

In humans, these enzymes play an important role in the catabolism of catecholamines with regulatory implications in neurotransmission mediated by adrenaline, dopamine, noradrenaline, and serotonin, as well as a neuroprotective role against xenobiotics that can cause excitotoxicity.² In humans, there are two isoforms of the enzyme, monoamine oxidase-A (MAO-A), which has physiological activity predominantly in the peripheral regions of the body, and monoamine oxidase B (MAO-B), which has physiological activity in the central nervous system.³

*e-mail: loranehage@gmail.com

Editor handled this article: Paula Homem-de-Mello (Associate)



In the field of pathophysiology, MAO-A dysregulation is associated with depression; however, positron emission tomography studies have shown a significant increase in MAO-B activity in patients with episodes of major depression.^{4,5} Furthermore, postmortem studies with individuals with schizophrenia showed that the gene expression of MAO-A and MAO-B was 45% above normal, highlighting that many MAO-B polymorphisms are recognized as susceptibility factors for schizophrenia.⁶

The isoform of MAO-A in Parkinson's disease is responsible for the decrease in dopaminergic levels, whereas MAO-B contributes to the pathophysiology of the condition by mediating the abnormal synthesis of gamma-aminobutyric acid (GABA) and hydrogen peroxide in astrocytes. In addition, reactive oxygen species are responsible for the suppression and degradation of dopaminergic neurons.⁷

In this context, and with a focus on MAO-B inhibitors, Carradori *et al.*⁸ present therapeutic indications of this pharmacological class for the treatment of Parkinson's disease, as a neuroprotective agent for Alzheimer's and Huntington's diseases, aiming to prevent oxidative stress caused by the Fenton reaction derived from the production of hydrogen peroxide of the enzymatic catalysis of MAO-B, as well as indication as a future treatment to quit smoking.

Moreover, Carradori *et al.*⁸ highlighted the importance of medicinal chemistry for pharmaceutical innovation in patent development, in which pharmacokinetic prediction methods based on physicochemical properties optimize the search and selection of successful candidates for new drugs.⁹

In this sense, medicinal chemistry offers alternatives to identify crucial elements for the planning and design of novel drugs. Computational methods aid in the identification of therapeutic targets, offer perspectives that enhance comprehension of the sites of interaction between ligands and proteins, and assist in the virtual screenings of potential new drug candidates through ligand-based or structure-based studies. Representing a highly valuable set of tools for the pharmaceutical industry because it drastically reduces the time and expenses associated with the discovery and development of novel drugs.^{10,11}

Thus, considering the significance of this protein as a pharmacological target for the treatment of central nervous system (CNS) disorders, this work aimed to search for compounds with selective MAO-B inhibitory features through computational methods considering the construction of a pharmacophoric model in the webserver PharmaGist¹² based on the features of 31 compounds with high inhibitory activity against MAO-B that were collected from the database BindingDB.¹³

Then, a pharmacophoric-based search was conducted in the platform ZincPharmer¹⁴ where 10,000 compounds were raised and used to build 10 conformers in the software OMEGA¹⁵ for each compound obtained.¹⁵ Followed by screenings with basis on structural and electrostatic similarity of the compounds to safinamide (a selective MAO-B inhibitor) using the software ROCS (Rapid overlay of chemical structures)^{16,17} and EON (Electrostatic similarity for lead-hopping),^{18,19} respectively, leading to the obtention of 1,000 compounds.

Subsequently, a molecular docking study using the software GOLD (Genetic Optimization for Ligand Docking)^{20,21} was performed to rank the compounds with the 110 highest scores to select those with results indicating a high probability of affinity to the target of the research. Moreover, contemplating the refinement of virtual screening aiming at selective MAO-B inhibitors with physical-chemical properties suitable for the development of pharmaceutical products. We evaluated the physical-chemical properties, predictive pharmacokinetics, and toxicity alerts of the compounds with the highest scores using the software QikProp^{22,23} and DEREK,^{24,25} and the webserver SwissADME.²⁶⁻²⁸

Finally, we reached 4 compounds with the best *in silico* results and evaluated their patterns of molecular interactions with MAO-B through molecular docking, and compared them to the *in silico* data of selective inhibitors with experimental results available in the literature. Noting that the reason behind the focus on selective MAO-B inhibitors was their clinical efficacy and safety compared with non-selective or MAO-A irreversible inhibitors that tend to present longer effects and serious interactions with drugs and food that lead to norepinephrine hyper stimulation.^{29,30}

Methodology

Research for MAO-B inhibitors

In order to create a suitable pharmacophoric model for virtual screening, we searched the BindingDB¹³ database using the descriptor "Monoamine oxidase B Inhibitors" with the goal of identifying the fundamental structural and physicochemical characteristics shared by ligands that exhibit strong inhibitory activity on MAO-B, as indicated by inhibitory concentration 50 (IC₅₀) values up to 1.00 nM.

In this sense, BindingDB is a database launched in 2000 that facilitates research on small compounds. It contains carefully selected experimental data from other databases, including PubChem, ChEMBL, PDSP Ki, and CSAR. Quantitative measurements of the affinity between proteins and ligands, such as IC₅₀, inhibition constant (K_i), half

maximal effective concentration (EC_{50}), and dissociation constant (K_d), as well as experimental characteristics, such as assay description and environmental variables like pH and temperature, which can be used as search filters.^{31,32}

Noting that 1,454,894 binding data for 7,082 protein targets and 652,068 small compounds were present in BindingDB in 2018³³ and that this quantity is currently much greater.

Determination of pharmacophore groups

Pharmacophore is a term that designates attributes of the spatial arrangement and physicochemical properties that are essential for the interaction of a molecule with a specific protein target, therefore, aiming to construct a pharmacophoric model for MAO-B based on the ligands obtained from BindingDB¹³ database, the webserver PharmaGist¹² was used to compare features as aromatic regions, hydrophobic groups, hydrogen donors and acceptors, as well as positively and negatively charged groups between the ligands, looking forward the most frequent attributes among the molecules aligned in a three-dimensional plane.

Thus, the pharmacophore regions found in the 31 hits collected in BindingDB¹³ were searched in the webserver PharmaGist¹² and subsequently visualized in the webserver ZincPharmer,¹⁴ in which a pharmacophore-based search was also conducted with the following filters: max hits by conf: 1; maximum hits *per* mole: 1; total molecules (hits): 10,000; root-mean-square deviation (RMSD): 1.5; molecular weight: 0 to 400 g mol⁻¹; rotatable links: 0 to 10, considering purchasable molecule database updated on 12/20/2014, resulting in 10,000 ligands.

Electrostatic and conformational correlation screening

10,000 ligands were gathered for the ZincPharmer search and sent to OMEGA^{15,34} from OpenEye Scientific to produce 10 conformers. The goal of these conformers was to assess potential rotational stereochemical properties in a three-dimensional plane that could have an impact on biological activity. After that, screening was done using the ROCS^{16,17} software with the 10 conformers of each ligand. This enabled the obtaining of molecules with structural similarity to safinamide. Noting that EON^{18,19} was used to assess electrostatic similarity among the ligands in screening, also considering safinamide as a MAO-B selective inhibitor standard.

Emphasizing that ROCS¹⁶ and EON¹⁸ are instruments that carry out inferential correlation analyses, assessed by means of the Tanimoto coefficient; molecules exhibiting

outcomes more akin to the safinamide exhibit values nearer to 1, whereas the most dissimilar molecules display values closer to 0. Then, a predictive study of the target and ligand interaction was performed on the 1000 molecules that yielded the best findings after the application of electrostatic and structural filters.

Screening by molecular docking

The ligands with structural and electrostatic similar to safinamide obtained in the previous research step were subjected to molecular docking in the software GOLD20-21 using a genetic algorithm to optimize docking times and increase the possibilities of determining the best fit.³⁵ Only the molecules ranking in the 110 best scores (including 2 safinamide conformers) remained in the study.

The molecular docking was conducted using a file with data from the crystal structure of human MAO-B in complex with zonisamide presenting resolution of 1.80 Å. This file is available at the Protein Data Bank (PDB) under the PDB-ID code 3PO7.

In the method adopted, the water molecules from the crystallography were eliminated, the FAD cofactor remained in the monomer A active site of the protein which was the sole area that was taken into consideration for docking. ChemPLP was the scoring function of choice. The redocking method was used to validate the results generated by GOLD, considering a root mean square deviation (RMSD) value equal to or less than 2 Å between the pose of zonisamide generated by GOLD and the pose of the ligand in the crystal structure.

After ranking the 110 best scores, the ligands' physicochemical characteristics were extracted with the use of the software QikProp, and evaluated according to Lipinski's rules considering a tolerance of just one violation.

Prediction of pharmacokinetic and toxicological properties

Looking forward a new drug reaching the clinical practice, the pharmacokinetic and toxicological behavior is an essential factor in determining dosage choices, schedules, adjustments, and treatment adequacy.³⁶⁻³⁹ As well as for planning the development of formulations that maximize bioavailability, increase metabolic stability through the synthesis of pro-drugs, delay of the drug release and absorption profile to prolong the pharmacological action, or even allow for the site-specific release of drugs, as in the case of enteral release tablets and capsules.^{40,41}

Thus, using the software QikProp from Schrödinger^{22,23} and DEREK from Lhasa,^{24,25} as well as SwissADME,²⁶⁻²⁸

pharmacokinetic and toxicological parameters of the compounds chosen in the molecular docking screening were assessed.

The compounds with any toxicity alerts based on Custom Prediction and Lhasa Predictions were rejected concerning the toxicological parameters assessed by DEREK.⁴²

Additionally, the descriptors permeability in Caco cells (log Caco), log MDCK (Madin-Darby Canine Kidney cells), percentage of oral absorption, quality of the human model of oral absorption, binding to human serum albumin (log KHSA), blood-brain barrier (log BB), number of metabolic reactions, activity in the central nervous system, and stars were taken into consideration for the pharmacokinetic predictions made in the QikProp²² program. Furthermore, the ability of the remaining compounds to inhibit CYP450 enzymes and to be transported by P-glycoprotein was assessed on SwissADME.²⁶⁻²⁸

The most promising ligands were those with a score value greater than that of safinamide, no toxicity alerts, and acceptable predictive pharmacokinetic data.

Concerning the computational tools used in this step of the research, QikProp is a software that can produce physicochemical and pharmacokinetic predictions from chemical structure data in SDF format.²²

DEREK is a software that generates models that enable the analysis of the structure-activity of molecules with input in mol (.mol), sketch (.skc) formats or .SDF (.sdf) following algorithms for automating toxicological predictions in the form of alerts.⁴² And SwissADME is a free webserver that provides free access to a variety of fast and reliable predictive models for physicochemical properties, pharmacokinetics, druggability according to medicinal chemistry parameters, with the presentation of results in in-house models such as iLOGP, Bioavailability Radar and BOILED-Egg.²⁸

Results and Discussion

This study employed an approach based on ligand aided by molecular docking followed by selection with a basis on desired properties for drug discovery and development, as summarized in Figure 1. The details on the results can be found in their respective topics below.

Pharmacophore-based virtual screening

Like high-throughput screening, virtual screening involves the use of computers to search and select molecules from large libraries that have records of biological activity, structural, and physicochemical data to identify the most promising hit, lead or drug candidates.

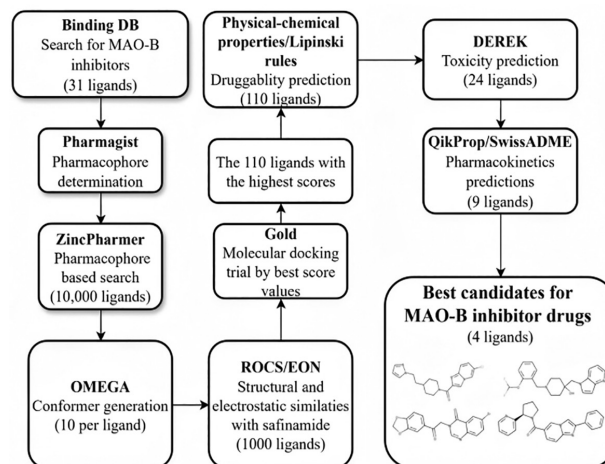


Figure 1. The process of selecting the best MAO-B inhibitor candidates for virtual screening involves a number of steps, including the selection of hit molecules in the BindingDB, pharmacophore-based search, structural and electrostatic similarity with the selective inhibitor safinamide, molecular docking-based prediction of affinity to MAO-B score, as well as predictive toxicological and pharmacokinetics, resulting in 4 molecules out of 10,000.

Thus, the study done was intended to look for inhibitors of MAO-B in the Binding DB database. It produced 7309 hits, out of which 31 were within the IC_{50} cutoff value of 1 mM and had a range of amplitude of 0.918 with a minimum value of 0.00820 mM.

These substances exhibit strong inhibitory activity against the specified target, as indicated by their low IC_{50} values. Emphasizing that every substance taken out of Binding DB showed experimental results from analyses using human MAO-B. However, it is important to highlight that enzyme kinetics and inhibition assays can present considerable variability due to the experimental procedures adopted, including substrate and product quantification methods, factors such as the influence of pH, ionic strength, allosteric regulation sites, cascade reactions, substrate concentration, and the concentration of reaction products with inhibitory or denaturing activity on the test enzyme.⁴³

Nevertheless, it is noteworthy that the molecules derived from Binding DB were examined using human MAO-B, as this lessens the difficulties resulting from structural variations that diminish the similarity between the human protein and the enzyme found in animal models or microbes.^{11,44} But, it ignores polymorphisms that affect enzymatic functionality, as well as the clinical presentation of neuropsychiatric disorders associated with MAO-B, and how responsive a patient is to treatment.⁴⁵⁻⁴⁸

The chemical structure, molecule's ID, IC_{50} and International Union of Pure and Applied Chemistry (IUPAC) name from the ligands obtained in the Binding DB database can be seen in Table 1.

A molecular alignment has been done with the

Table 1. Ligands obtained in the BindingDB database with their structures, IDs from PubChem, ChEMBL and BindingDB, IC₅₀, and IUPAC name

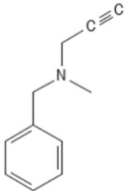
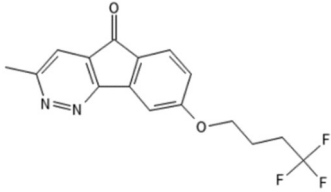
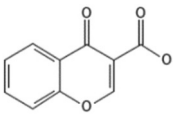
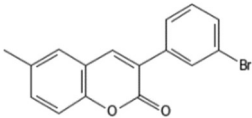
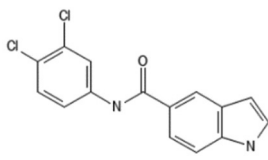
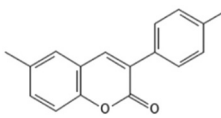
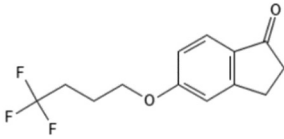
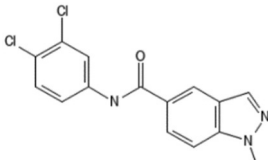
Structure	ID PubChem / ChEMBL / BindingDB	IC ₅₀ / nM	IUPAC name
<p>Ligand 1</p> 	CID 4688 ChEMBL673 BDBM50172756	0.00820	<i>N</i> -benzyl- <i>N</i> -methylprop-2-yn-1-amine
<p>Ligand 2</p> 	CID 10314028 ChEMBL348961 BDBM501211688	0.0140	3-methyl-8-(4,4,4-trifluorobutoxy)indeno[1,2- <i>c</i>]pyridazin-5-one
<p>Ligand 3</p> 	CID 181620 ChEMBL315361 BDBM50131081	0.0480	4-oxo-4 <i>H</i> -1-benzopyran-3-carboxylic acid
<p>Ligand 4</p> 	CID 46895501 ChEMBL4129303 BDBM50276359	0.134	3-(3-bromophenyl)-6-methylchromen-2-one
<p>Ligand 5</p> 	CID 63718419 ChEMBL3319268 BDBM50046943	0.227	<i>N</i> -(3,4-dichlorophenyl)-1 <i>H</i> -indole-5-carboxamide
<p>Ligand 6</p> 	CID 13441539 ChEMBL1835228 BDBM50355323	0.310	6-methyl-3-(4-methylphenyl)chromen-2-one
<p>Ligand 7</p> 	CID 11708681 ChEMBL414637 BDBM50121685	0.318	5-(4,4,4-trifluorobutoxy)-2,3-dihydroindeno-1-one
<p>Ligand 8</p> 	CID 77844667 ChEMBL3319256 BDBM50046866	0.386	<i>N</i> -(3,4-dichlorophenyl)-1-methylindazole-5-carboxamide

Table 1. Ligands obtained in the BindingDB database with their structures, IDs from PubChem, ChEMBL and BindingDB, IC₅₀, and IUPAC name (cont.)

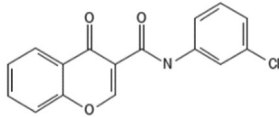
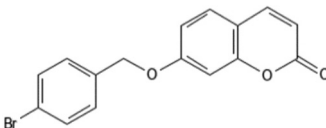
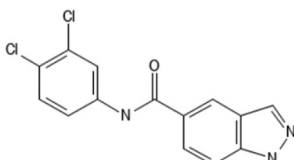
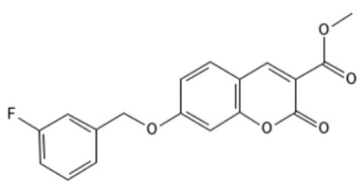
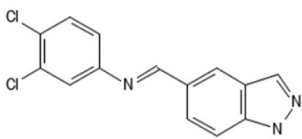
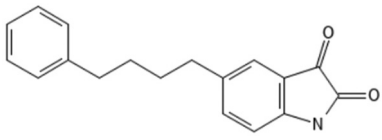
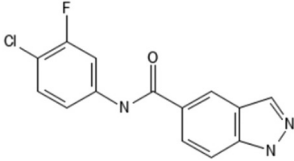
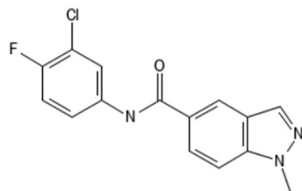
Structure	ID PubChem / ChEMBL / BindingDB	IC ₅₀ / nM	IUPAC name
<p>Ligand 9</p> 	CID 132941420 ChEMBL4206812 BDBM5045319	0.400	<i>N</i> -(3-chlorophenyl)-4-oxochromene-3-carboxamide
<p>Ligand 10</p> 	CID 2629406 ChEMBL4068321 BDBM50259594	0.500	7-[(4-bromophenyl)methoxy]chromen-2-one
<p>Ligand 11</p> 	CID 77844601 ChEMBL3319244 BDBM50046950	0.586	<i>N</i> -(3,4-dichlorophenyl)-1 <i>H</i> -indazole-5-carboxamide
<p>Ligand 12</p> 	CID 76314457 ChEMBL3121793 BDBM50496171	0.588	methyl 7-[(3-fluorophenyl)methoxy]-2-oxochromene-3-carboxylate
<p>Ligand 13</p> 	CID 77844723 ChEMBL3319272 BDBM50046948	0.612	<i>N</i> -(3,4-dichlorophenyl)-1-(1 <i>H</i> -indazol-5-yl)methanimine
<p>Ligand 14</p> 	CID 50994176 ChEMBL1642678 BDBM50334292	0.660	5-(4-phenylbutyl)-1 <i>H</i> -indole-2,3-dione
<p>Ligand 15</p> 	CID 77844664 ChEMBL3319247 BDBM50046878	0.661	<i>N</i> -(4-chloro-3-fluorophenyl)-1 <i>H</i> -indazole-5-carboxamide
<p>Ligand 16</p> 	CID 77844718 ChEMBL4061639 BDBM50232425	0.662	<i>N</i> -(3-chloro-4-fluorophenyl)-1-methylindazole-5-carboxamide

Table 1. Ligands obtained in the BindingDB database with their structures, IDs from PubChem, ChEMBL and BindingDB, IC₅₀ and IUPAC name (cont.)

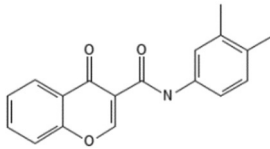
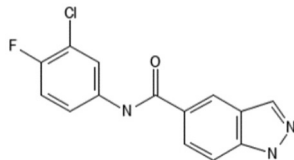
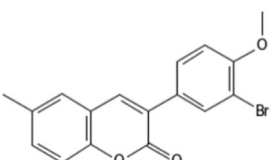
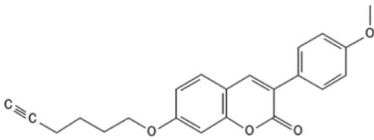
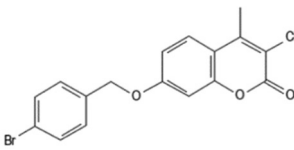
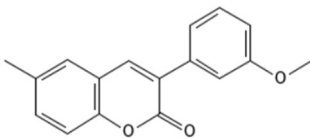
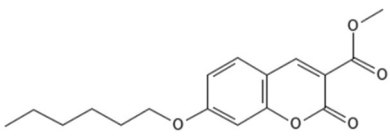
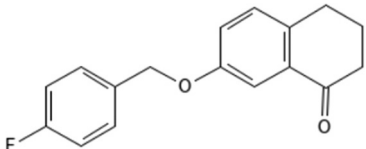
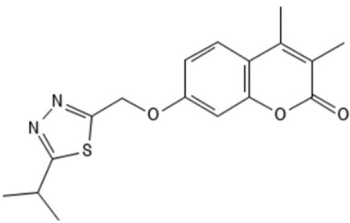
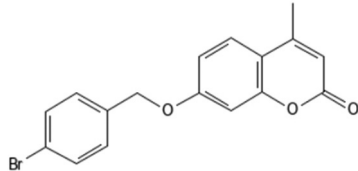
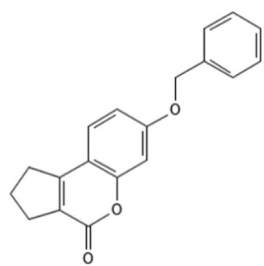
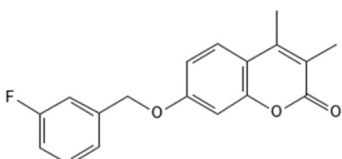
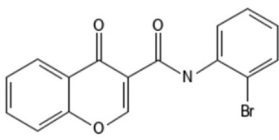
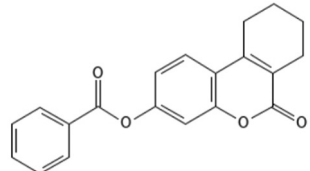
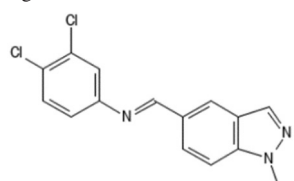
Structure	ID PubChem / ChEMBL / BindingDB	IC ₅₀ / nM	IUPAC name
	CID 132941421 ChEMBL4209203 BDBM50453020	0.670	<i>N</i> -(3,4-dimethylphenyl)-4-oxochromene-3-carboxamide
	CID 77844663 ChEMBL3317469 BDBM50046879	0.678	<i>N</i> -(3-chloro-4-fluorophenyl)-1 <i>H</i> -indazole-5-carboxamide
	CID 46847345 ChEMBL1835231 BDBM50355325	0.740	3-(3-bromo-4-methoxyphenyl)-6-methylchromen-2-one
	CID 76318046 ChEMBL31211792 BDBM50355325	0.770	7-hex-5-ynoxy-3-(4-methoxyphenyl)chromen-2-one
	CID 134816193 ChEMBL4079843 BDBM50259630	0.800	7-[(4-bromophenyl)methoxy]-3-chloro-4-methylchromen-2-one
	CID 44622873 ChEMBL570731 BDBM50300895	0.800	3-(3-methoxyphenyl)-6-methylchromen-2-one
	CID 76336202 ChEMBL3121865 BDBM50496179	0.875	methyl 7-hexoxy-2-oxochromene-3-carboxylate
	CID 105624050 BDBM166634	0.890	7-[(4-fluorophenyl)methoxy]-3,4-dihydro-2 <i>H</i> -naphthalen-1-one

Table 1. Ligands obtained in the BindingDB database with their structures, IDs from PubChem, ChEMBL and BindingDB, IC₅₀, and IUPAC name (cont.)

Structure	ID PubChem / ChEMBL / BindingDB	IC ₅₀ / nM	IUPAC name
	CID 179342 ChEMBL19004 BDBM50252506	0.900	3,4-dimethyl-7-[(5-propan-2-yl-1,3,4-thiadiazol-2-yl)methoxy]chromen-2-one
	CID 886539 ChEMBL4097867 BDBM50259595	0.900	7-[(4-bromophenyl)methoxy]-4-methylchromen-2-one
	CID 561354 ChEMBL142799 BDBM50409101	0.900	7-phenylmethoxy-2,3-dihydro-1H-cyclopenta[c]chromen-4-one
	CID 807313 ChEMBL108697 BDBM50409097	0.912	7-[(3-fluorophenyl)methoxy]-3,4-dimethylchromen-2-one
	CID 155568351 ChEMBL4591558 BDBM50535909	0.912	<i>N</i> -(2-bromophenyl)-4-oxochromene-3-carboxamide
	CID 2235896 ChEMBL1213297 BDBM36478	1.00	(6-oxo-7,8,9,10-tetrahydrobenzo[c]chromen-3-yl) benzoate
	CID 77844772 ChEMBL3319273 BDBM50046949	1.00	<i>N</i> -(3,4-dichlorophenyl)-1-(1-methylindazol-5-yl)methanimine

IC₅₀: half maximal inhibitory concentration.

31 compounds extracted from Binding DB to identify the pharmacophoric areas in the Web Server PharmaGist. The outcome showed that two aromatic areas and a hydrogen acceptor region were common in 29 out of the 31 compounds aligned. Highlighting that compounds **1** and **7** did not take part in the alignment because of high structural variation concerning the other substances.

The pharmacophoric regions determined in Web Server PharmaGist can be seen in Figure 2.

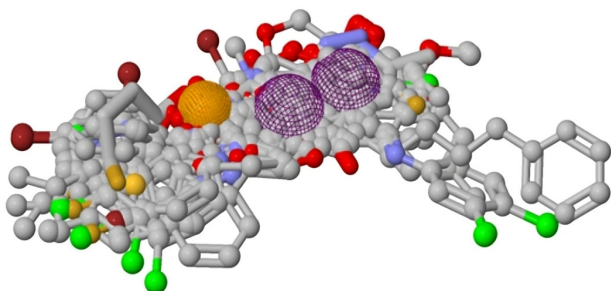


Figure 2. The pharmacophoric model, which was constructed using PharmaGist, shows two structural and physical-chemical characteristics among 29 hits that were taken from BindingDB; two aromatic sections are shown in purple, and a hydrogen acceptor region is shown in orange.

Although the pharmacophoric regions identified in this study differ from those found by Gritsch *et al.*,⁴⁹ who reported three hydrogen acceptor regions, a hydrophobic region, and an aromatic ring, as well as from Boppana *et al.*,⁵⁰ who found a hydrogen acceptor region, a hydrogen donor region, and an aromatic ring, they do corroborate with the findings of Souza *et al.*⁵¹ All the examples, however, clearly have an aromatic ring with at least one hydrogen acceptor area present. Therefore, there is consistency between the results obtained and the literature on this topic.

Generation of conformers and sorting by electrostatic and structural similarity

Following the creation of the pharmacophoric model, 10,000 hits were found through a search on the ZincPharmer¹⁴ web server. These hits were then used to produce 10 conformers using the software Omega¹⁵ to assess the impact of stereochemical and rotational properties in three-dimensional plane over the biological activity of the chosen molecules. Next, using the software programs ROCS,¹⁶ 1000 ligands were filtered based on their structural and electrostatic similarity to safinamide.

The software OMEGA was incorporated into the research workflow due to the work of Perola and Charifson.⁵² extensive analysis of the energetic and conformational variations resulting from ligand-target

protein interaction. They discovered a strong correlation between ligand flexibility and tension energy with binding affinity to the target protein, which allowed for the identification of molecules in conformations more likely to exhibit desired bioactivity.

Additionally, the software EON¹⁸ was chosen because electrostatic parameters affect the ligand-target interaction, as shown by Boström *et al.*,⁵³ who found that the substance 5-(4-piperidyl)-3-isoxazole (4-pyol) has potential therapeutic applicability for treating coagulation disorders through electrostatic comparison via EON with tranexamic acid. Concurrently, the ROCS software enables screenings centered on structural elements pertinent to the intended impact and structural comparisons with ligands whose biological activity is previously established.^{17,54}

In this regard, Crisan *et al.*⁵⁵ report positive outcomes from *in silico* studies for the screening of MAO-B inhibitors using the OMEGA, EON, and ROCS. They made conformer banks with molecules compared with safinamide using the software EON and ROCS, which helped discover the natural product cardamomin ((*E*)-1(2,4-dihydroxy-6-methoxyphenyl)-3-phenylprop-2-em-1-one) and reuse of monobenzene and fenamisal for Parkinson's disease treatment.

Therefore, it is expected that the 1000 ligands screened in this study using the OMEGA, EON, and ROCS tools exhibit pharmacodynamic properties similar to those of safinamide, a reversible MAO-B inhibitor with a more favorable side effect profile than irreversible inhibitors like rasagiline and selegiline, which inactivate MAO-B for an extended period, resulting in the occurrence of serious side effects as well as drug interactions that may cause cardiac side effects due to raises levels of catecholamines.⁵⁶

Screening by molecular docking

The 1000 ligands that were selected based on their electrostatic potential and structural resemblance to safinamide underwent molecular docking assay using the target 3po7 in the software GOLD. This approach led to the extraction of 110 molecules (including 2 safinamide molecules), whose scores varied from 66.93 to 101.2 with a range of 34.27, average of 90.44, and median of 90.59.

The redocking method was used to validate the *in silico* assay. This method assesses the ability of the software to replicate the initial pose of the ligand co-crystallized with the target protein; RMSD values below 1 are regarded as excellent, values between 1 and 2 as good, values between 2-3 as moderate, and values above 3 as incorrect.⁵⁷

The best pose determined by GOLD for zonisamide and its comparison with the crystal structure are shown in Figure 3. The RMSD achieved was 0.428 Å.

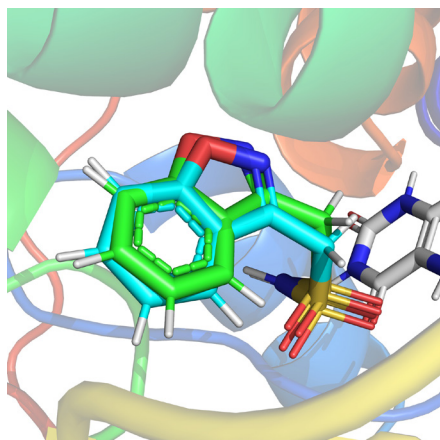


Figure 3. Overlap between the co-crystallized molecule (blue) and the best pose generated by GOLD (green), FAD co-factor (white), RMSD = 0.428 Å.

The three-dimensional coordinates of the MAO-B used in the validation procedure were $x = 53.32$, $y = 153.71$, and $z = 25.55$ with a radius of 8.8 Å, and they designate the orthosteric site of the protein, a region where reversible and selective inhibitors as zonisamide and safinamide interact with MAO-B,⁵⁸ enabling the use of molecular docking as a strategy to identify interactions between an unknown ligand and MAO-B residues to estimate binding affinities and potential biological activity.⁵⁹

The average score achieved by the two safinamide molecules was 89.57 (one in a conformation taken from the PDB and the other from OMEGA). And this average was used as a cutoff value for the selection of ligands with suitable toxicological and pharmacokinetic properties for the study, and the discovery of new MAO-B inhibitors.

Emphasizing that in this virtual screening, the ligands with scores higher than 89.57 presented desired predictions of association/affinity with MAO-B through an empirical approach (ChemPLP score function) that considers hydrogen bonds, numerous potentials for modeling van der Waals interactions, repulsion potentials, as well as steric complementarity with a low computational cost.⁶⁰⁻⁶²

The 110 ligands that had been screened by molecular docking were then evaluated for their physicochemical characteristics in an effort to weed out molecules that were not acceptable for the development of oral formulations.

Physical-chemical properties

Correlations between physical-chemical properties and biological activity/toxicity have been found in several

medicinal chemistry investigations into the chemical space of ligands of interest. These correlations are important for the screening of new drug candidates and are also helpful in absorption, distribution, metabolism, excretion and toxicity (ADMET) optimization campaigns, modulating pharmacological potency, and repurposing known molecules with promising applications for the treatment of a particular disease.^{63,64}

In this case, descriptive analysis and comparison with druggability metrics were conducted accounting with molecular weight values, frequencies of acceptor and donor groups of hydrogen interactions, and octanol/water partition coefficient among the 110 ligands screened by molecular docking.

The results of the descriptive analysis indicate that the ligands had more hydrogen acceptor groups than hydrogen donor groups, presenting average of 0.83, median of 1 and range of 3.25 (minimum = 0; maximum = 3.25). In addition, the frequency of hydrogen acceptor groups observed among the ligands had an average of 5.9, median of 5.50, and the range between the minimal value (2.25) and the maximum (10.5) was 8.2.

Regarding the octanol/water partition coefficient, the average achieved among the ligands was 3.59, with median of 3.57, and range of 8.3 (minimum = -1.18; maximum = 7.13). While the molecular weight among the ligands showed a range of 196.24, with a minimum value of 303.35 and a maximum value of 499.59. The average was 359.02 g mol⁻¹, with a median value of 355.41 g mol⁻¹.

Thus, considering passive transport by diffusion through the biological barriers of the body, Lipinski's rule of five recommends that a molecule have less than 5 hydrogen donor groups and less than 10 acceptor groups, an octanol/water partition coefficient that does not exceed 5, and a molecular weight inferior to 500 Da in order to present satisfactory oral absorption.⁶⁵⁻⁶⁷ Therefore, it was found that 16 ligands were over the cutoff value for the octanol/water partition coefficient, 2 ligands violated the maximum number of hydrogen donor groups, and none violated the molecular weight parameter. Noting that between the ligands with violations of Lipinski's rules, none of them violated more than one rule, so all the ligands proceeded to the next *in silico* assays.

In conclusion, the descriptive physical-chemical analysis of the ligands evaluated reveals promising candidates for further research. In this context, possible perspectives applicable to the ligands obtained by molecular docking screening, as well as for the pharmacophoric model created are ADMET optimization through: (i) bioisosterism, where isosteres (functional groups with similar shape and electronic properties) replace part of the

ligands as proposed structural modifications to explore structure-activity relationship features of novel substances⁶⁸ on MAO-B; and (ii) structural simplification aiming at new compounds from large lead ones.⁶⁹

Prediction of toxicological properties

The phenomenon known as toxicity is the result of an organism being exposed to chemicals. Usually, it depends on the dose and duration of exposure and can show up differently among cell types/lineages, developmental stages, or physiological states of the organism. Additionally, the chemical agents can interact with various molecular targets and may cause cellular or tissue damage or dysfunction, whose reversibility depends on the degree of impairment in the biological system.⁷⁰⁻⁷⁴

In this context, the computational techniques enable accurate screening of numerous drugs in a short amount of time and at comparatively lower costs than *in vitro* and *in vivo* models. This contributes to lessening the requirement for animal models, which is a significant ethical concern in biomedical research.⁷⁵ Moreover, it also makes it possible to assess various forms of toxicity extensively, which aids in the comprehension of potential toxicity-related mechanisms of action.⁷⁶

Therefore, in this investigation, the following toxicity alerts were taken into account using DEREK's computational toxicological prediction tests: carcinogenicity, mutagenicity, chromosome damage, teratogenicity, hERG channel inhibition, nephrotoxicity, hepatotoxicity, skin sensitization, photo allergenicity, mitochondrial dysfunction, effect of cyanide type, thyroid toxicity, modulation of androgen receptors, modulation of glucocorticoid receptors and methemoglobinemia.

Out of all the 110 ligands screened by molecular docking, only 24 ligands (64, 276, 292, 309, 325, 354, 365, 401, 412, 451, 596, 627, 698, 720, 775, 781, 824, 843, 903, 939, 973, 984, 986, and 994) were not associated with any toxicity alert in the *in silico* tests. Their ZincPharmer ID and chemical structure can be seen in Table 2.

These ligands were then subjected to *in silico* pharmacokinetic prediction assessments. It should be mentioned that the standard molecule of the study, safinamide, had two warnings about toxicity: one relating to the blockage of hERG channels linked to the type III pharmacophore, and the other about nephrotoxicity related to the presence of a halogenated benzene group.

However, this alert of cardiotoxicity found in safinamide can be interpreted as null, because selective MAO-B inhibitors are not linked to the risk of hypertensive crisis.⁷⁷

Table 2. Ligand with absence of toxicity alerts in the *in silico* analysis, their ZincPharmer ID and chemical structure

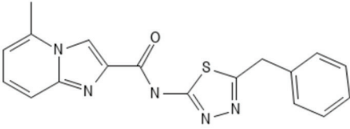
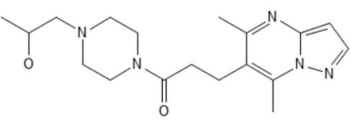
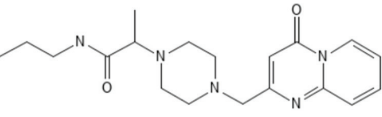
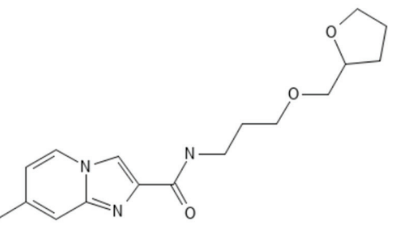
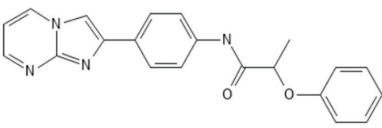
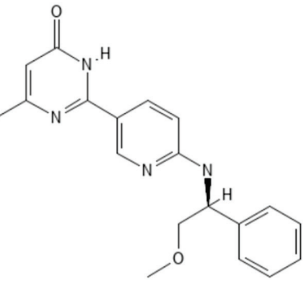
Ligand	Structure and ZincPharmer ID	Ligand	Structure and ZincPharmer ID
64	 ZINC40159782	276	 ZINC69844252
292	 ZINC29522538	309	 ZINC44895437
325	 ZINC4950251	354	 ZINC91981893

Table 2. Ligand with absence of toxicity alerts in the *in silico* analysis, their ZincPharmer ID and chemical structure (cont.)

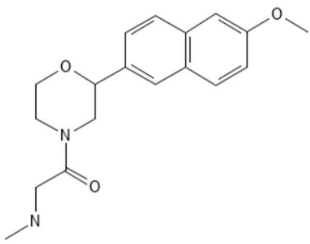
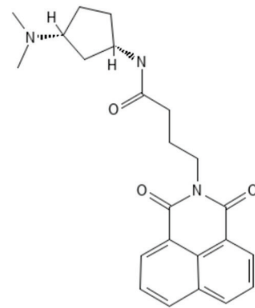
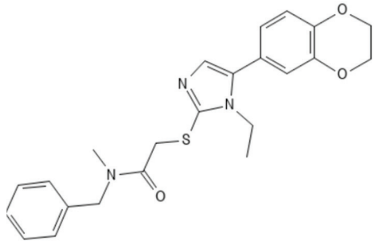
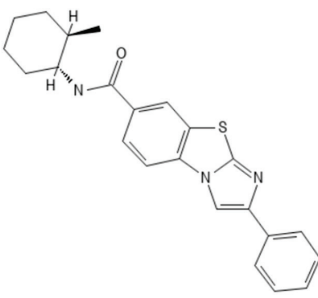
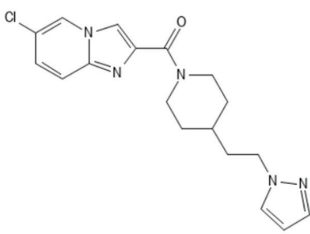
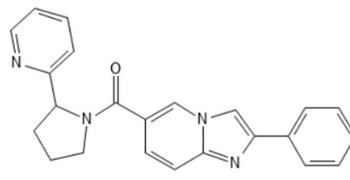
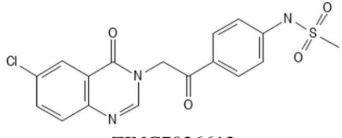
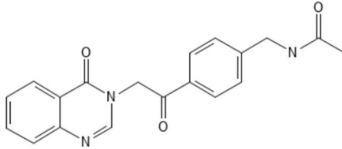
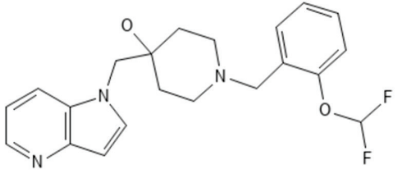
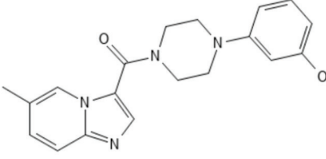
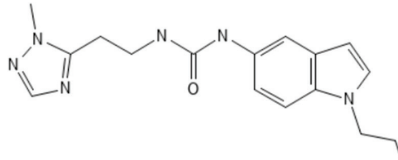
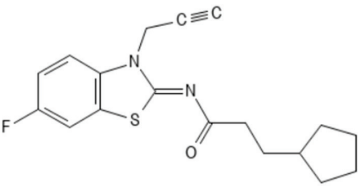
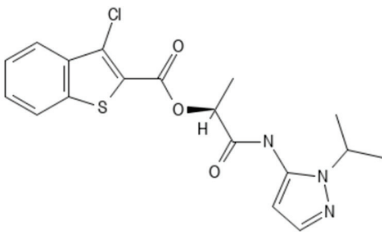
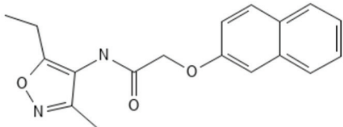
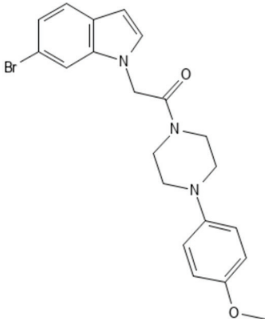
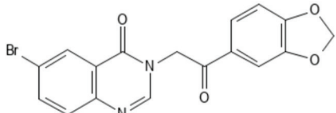
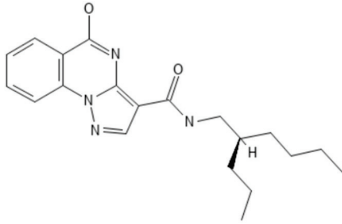
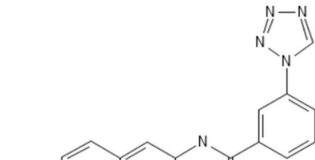
Ligand	Structure and ZincPharmer ID	Ligand	Structure and ZincPharmer ID
365	 ZINC71765131	401	 ZINC93983433
412	 ZINC06973093	451	 ZINC06748767
596	 ZINC77392807	627	 ZINC82148218
698	 ZINC7026612	720	 ZINC07268854
775	 ZINC19348852	781	 ZINC90094627
824	 ZINC88380864	843	 ZINC38873793

Table 2. Ligand with absence of toxicity alerts in the *in silico* analysis, their ZincPharmer ID and chemical structure (cont.)

Ligand	Structure and ZincPharmer ID	Ligand	Structure and ZincPharmer ID
903	 <p>ZINC07652641</p>	939	 <p>ZINC89393411</p>
973	 <p>ZINC20731299</p>	984	 <p>ZINC07392264</p>
986	 <p>ZINC84826429</p>	994	 <p>ZINC72247560</p>

Furthermore, Jost⁷⁸ reviewed the literature concerning the clinical outcomes and adverse effects of MAO-B inhibitors and found no significant influence in tyrosine depletion and no negative influence of safinamide on the duration of the ventricular action potential (QT intervals), also noted safety when used in conjunction with serotonin and norepinephrine reuptake inhibitors and selective serotonin reuptake inhibitors in individuals with Parkinson's disease and depression, and no reports of the occurrence of serotonergic syndrome, as well as no events concerning nephrotoxicity

Within this framework, Hemmerich and Ecker⁷⁹ highlight that the primary obstacles to the predictive potential of *in silico* techniques for toxicity assessment are data accessibility, model interpretability, and a certain amount of intrinsic uncertainty in computational tools. Moreover, DEREK's main limitation of the outputs is the capacity for human integration of various structural, physicochemical rules and biological data into programming.³⁴

Noting that the halogenated benzene alarm is valid in safinamide ((2S)-2-[4-[(3-fluorobenzyl)amino]phenyl]propanamide) because it has a fluorine atom in its structure, which demonstrates the need for future investigations that assist in the discrimination of structurally similar molecules, where the presence of certain functional groups represents a determinant of toxicity. As in the case of carbamazepine and oxycarbamazepine, where the first has a double bond between carbons 10 and 11 that requires oxidation through reactions catalyzed by CYP450 to form the intermediate metabolite 10,11-epoxidecarbamazepine, which is an extremely reactive compound capable of reacting with nucleophilic sites of proteins and nucleic acids, while oxycarbamazepine has a ketone group in position 10, which is reduced to a hydroxyl group during its metabolism to form the non-toxic intermediate metabolite 10-monohydroxy-oxycarbamazepine and the final product 10,11-dihydroxy-oxycarbamazepine after hydroxylation of the carbon at position 11.⁸⁰

Pharmacokinetic predictions

The ligands **309**, **325**, **412**, **596**, **627**, **639**, **775**, **903** and **984** and the standard molecule safinamide presented satisfactory results in the pharmacokinetic predictions of absorption, distribution and metabolism carried out in the QikProp, considering the following descriptors stars, human oral absorption, percentage of human oral absorption, permeability in Caco cells (log Caco) and in MDCK cells (log MDCK), metabolic reactions, binding to human serum albumin (log KHSA), central nervous system activity (CNSa) and permeability in the blood-brain barrier (log BB).

The results of ligands with satisfactory results in screening based on pharmacokinetic prediction can be seen in Table 3.

The results from QikProp, according to Ioakimidis *et al.*⁸¹ strongly correlate with experimental data on octanol-water partition coefficient (log P), aqueous solubility (log S), adiabatic and vertical ionization potentials, and dipole moments. The software generates results that follow trends expected in experimental permeability data of Caco-2 and MDCK cells, but it biases the results in terms of blood-brain barrier penetration and predictions of central nervous system activity because it takes into account a compilation of compounds not expected to penetrate the blood-brain barrier.

In this sense, the parameter predicting activity in the central nervous system presented a value of 0 for safinamide, highlighting that it is a drug with known activity at the central level, corroborating Ioakimidis *et al.*,⁸¹ And only ligand **775** showed any predictive value for CNSa. Therefore, proper *in vivo* experimentation is needed to characterize the quality and extension of the activity of the ligand over the CNS.

Concerning the parameter stars, the results obtained suggest high reliability of the data obtained by indicating chemical similarity between the ligands screened with known drugs from the QikProp database.⁸²

Proceeding to other parameters of analysis, the term “absorption” refers to the process by which a drug enters the bloodstream after administration. In this context, the physical-chemical results indicate that the nine compounds under analysis have properties that are advantageous for oral absorption because they follow the Lipinski’s guidelines. However, according to Benet *et al.*,⁸³ Lipinski’s guidelines are only predicated on physicochemical characteristics pertaining to the passive passage of molecules across cell membranes.

Thus, the software Qikprop was used to predict the permeability in Caco-2 and MDCK cells because substances pass through biological membranes involving a variety of lipids (such as triglycerides and cholesterol rather than just octanol and water) and transporters that affect the levels of drug absorption through both active transport and facilitated diffusion.^{84,85}

In the software, the parameter human oral absorption can be expressed categorically as 1, 2, or 3, which stands for low, medium, and high absorption, respectively. The parameter percentage of oral absorption can present values below 25 that indicate a low percentage of oral absorption in humans, while values above 80 indicate a high percentage of oral absorption. While cellular permeability in Caco-2 and MDCK cells is low when these parameters present values below 25, and high when above 500.⁸⁶

Thus, beyond the process of absorption, a drug candidate with action in the CNS needs to cross the space related to adheren junctions and occluding zones of endothelial cells, which restrict the passage of endogenous and exogenous

Table 3. *In silico* pharmacokinetic predictions of the ligands screened with QikProp; permeability in Caco cells (log Caco) and in MDCK cells (log MDCK); human oral absorption (HOA); percentage of human oral absorption (HOA%); permeability in the blood-brain barrier (log BB); binding to human serum albumin (log KHSA); metabolic reactions, central nervous system activity (CNSa), and Stars

Ligand	Log Caco2	Log MDCK	HOA	HOA / %	Log BB	Log KHSA	Metabolic reactions	CNSa	Stars
Safinamide	116.708	179.65	3	75.653	-0.467	-0283	6	0	0
325	1614.12	830.04	3	100	-0.541	0.461	3	0	1
412	3075.46	3368.49	3	100	-0.112	0.328	2	0	0
984	1147.14	1514.60	3	91.97	-0.317	-0.764	2	0	0
903	1675.97	2531.69	3	100	-0.354	0.548	2	0	0
775	833.82	1363.60	3	100	0.349	0.773	5	1	0
309	2908.44	1568.60	3	100	-0.446	-0.123	3	0	0
596	1262.94	1575.19	3	100	-0.457	-0.110	0	0	0
627	3318.46	1808.93	3	100	-0.011	0.564	3	0	1
939	1650.99	850.50	3	100	0.556	0.304	4	0	0

molecules through the blood-brain cell barrier, without major limitations, preferably presenting low polar surface area, an octanol/water partition coefficient of at least 1.5, and low polar surface area. If not, active transport mechanisms mediated by membrane proteins will be required, as in the case of cerebral transport of glucose and other nutrients.⁸⁷

Noting that in the CNS, cerebrospinal fluid replaces blood in its function. This fluid is formed in the choroid plexus, a structure found in the cerebral ventricles, where a simple epithelium carrying several membrane transporters for nutrients, drugs, as well as their metabolites, can transport these substances from the blood to the cerebrospinal fluid or from the CNS to the blood. As the OATP1A2 transporter, a protein that permits the entry of substances of high polarity into the CNS, such as triptans, a class of drugs used to treat migraines.⁸⁸

Besides, the kinetics of drugs in the CNS involves an equilibrium between the concentration of free drug available to interact with its pharmacological target and the concentration of drug bound to plasma proteins, where high affinity to these proteins decreases the concentration of drug in the cerebrospinal fluid. Furthermore, in this context, high lipophilicity contributes to high permeability across the blood-brain barrier but with less specificity of distribution between the body tissues.⁸⁹

Thus, the pharmacological effect depends on the time required for the drug to reach the state of dynamic equilibrium between the blood and the cerebrospinal fluid, which along with the variables mentioned above, can also be affected by a wide variety of transporters including P-glycoprotein, Breast Cancer Resistance Protein (BCRP) proteins, multidrug resistance-type efflux proteins that prevent some drugs from reaching therapeutic concentrations in the CNS.⁹⁰

In this context, log K_hSA is a parameter that predicts the binding profile of molecules to serum albumin, where

values from -1.5 to 1.5 are ideal for drug candidates, while the parameter log BB presents predictive values for blood-brain barrier penetrability within the range of -3 to 1.2.⁹¹ Therefore, considering the distribution parameters analyzed, the selected ligands have appropriate predictive characteristics to reach the CNS. Additionally, only ligands **309**, **325**, **412**, and **775** presented positive results as substrates for P-glycoprotein.

Following to the parameters concerning metabolism, QikProp has the descriptor number of metabolic reactions, which is used to identify metabolic barriers that limit the ability of the test substance to reach the active site once it enters the bloody circulation, thereby providing an estimate of the steps involved in the biotransformation process. According to Ntie-Kang *et al.*⁹¹ and Fatima *et al.*,⁹² values in the range of 1 to 8 are ideal for screening purposes. Safinamide exhibited six distinct potential reactions, whereas the number of reactions ranged between 0 and 5 for the ligands under study.

Moreover, inhibitory activity of CYP450 enzymes was assessed using the webserver SwissADME encompassing isoforms from the CYP1, CYP2, and CYP3 families, which are enzymes accountable for the metabolism of roughly 80% of drugs used in clinical practice.⁹³ The isoforms evaluated were CYP1A2, CYP2C19, CYP2C9, CYP2D6, and CYP3A4.

The results obtained in SwissADME predicting the inhibition of CYPs and substrate for P-glycoprotein are shown in Table 4.

CYP inhibition increases the half-life of certain drugs due to the inhibition of metabolic transformations required for their elimination, consequently contributing to the occurrence of adverse effects and toxicity.⁹³

In this context, our results indicate ligands **984**, **903**, **775**, **627**, and **939** can inhibit the metabolism of drugs such as clozapine, caffeine, fluvoxamine, imipramine, olanzapine,

Table 4. Prediction of CYPs inhibition and substrate for P-glycoprotein

Ligand	Substrate for P-glycoprotein	CYP450 inhibitor				
		CYP1A2	CYP2C19	CYP2C9	CYP2D6	CYP3A4
Safinamide	no	no	yes	no	yes	yes
325	yes	no	no	no	no	yes
412	yes	no	yes	yes	yes	yes
984	no	yes	yes	yes	no	yes
903	no	yes	yes	yes	no	yes
775	yes	yes	yes	no	yes	yes
309	yes	no	yes	no	yes	no
596	no	no	yes	yes	yes	yes
627	yes	yes	yes	yes	yes	yes
939	no	yes	yes	yes	yes	yes

and zileuton due to CYP1A2 inhibition; ligands **412**, **984**, **903**, **775**, **309**, **596**, **627**, and **939** inhibit the metabolism of citalopram, omeprazole, phenytoin, and phenobarbital because of CYP2C19 inhibition; ligands **412**, **984**, **903**, **775**, **309**, **596**, **627**, and **939** interfere with the metabolism of carvedilol, celecoxib, glipizide, ibuprofen, irbesartan, and losartan by inhibiting CYP2C9; ligands **412**, **775**, **309**, **596**, **627**, and **939** inhibit the metabolism of amitriptyline, paroxetine, fluoxetine, carvedilol, metoprolol, haloperidol, donepezil, risperidone, codeine, and tramadol due inhibition of CYP2D6; while ligands **325**, **412**, **984**, **903**, **775**, **309**, **596**, **627**, and **939** inhibit the metabolism of alprazolam, diazepam, amlodipine, cyclosporin, atorvastatin, simvastatin, sildenafil, zolpidem and verapamil due to CYP3A4 inhibition.^{94,95}

In this instance, *in silico* analysis helps to predict aspects related to clinical practice such as the identification of potential drug-drug pharmacokinetic interactions, i.e., when one drug modifies the fluctuations in the plasma concentrations of another by influencing the absorption, distribution, metabolism, and elimination when both are administrated simultaneously.⁹⁶ Noting that it is imperative to underscore that the metabolism of drugs entails the involvement of enzymes apart from CYPs.⁸⁴

Potential candidates for MAO-B inhibitor drugs

The scores and interaction profiles of the ligands with the target residues were compared with those of the standard molecule (safinamide) in an attempt to aid in the selection of ligands with the best interaction profiles with MAO-B. Safinamide had an average score of 89.57 and interacted with the co-factor FAD600 as well as the residues Leu164, Gln206, Try435, Tyr398, Phe343, Leu171, Cys172, Tyr326, Ile199, and Ile316.

The ligands **627**, **596**, **775**, and **984** were elected as the most promising because they presented scores higher than

safinamide. Emphasizing that there was agreement on the interaction between the residues found in our safinamide molecular docking and the experimental crystallography data published by Binda *et al.*,⁹⁷ where the only differences found were for the residues Leu164 in the molecular docking and Phe103 and Tyr60 in the crystallography data.

The interaction profiles and the scores of the ligands **596**, **627**, **775**, and **984** can be seen in Table 5.

MAO-B has three functional domains in its structure: the aromatic cage consisting of Try398, Tyr435, and the co-factor FAD; and the substrate entry site that is separated from the substrate binding site by residues Phe168, Leu171, Ile199, and Try326. The substrate binding site is made up of residues Leu171, Tyr188, Tyr326 and Phe343; while the residues Gly58, Tyr60, Ile60, Gln206, Tyr326, and Cys397 belong to the active site of MAO-B.⁹⁸⁻¹⁰⁰

According to Reyes-Parada *et al.*,¹⁰¹ based on crystallography data and quantitative structure activity relationship studies, the Gln206 residue is relevant for maintaining the spatial orientation of the FAD co-factor in the active site as well as the orientation of residues that interact with ligands. Likewise, residues Tyr435, Tyr398, and Leu171 play important roles in guiding and stabilizing the binding of substrates and inhibitors in MAO-B, and residue Ile199 acts as a gate between these cavities. This makes the residues Try435, Tyr398, Leu171, and Ile199 relevant to the structure and functionality of MAO-B, therefore, they represent promising targets for the inhibitory activity and inhibitors selection. Moreover, it is noteworthy that residues Ile199 and Tyr326 are reported as essential for inhibitor selectivity.^{90,91}

In this context, the results obtained show the interactions of the ligands analyzed with the domains of the active site, aromatic cage, entry site, and substrate binding site, which are domains relevant for selective enzymatic inhibition, as seen in Figure 4.

Table 5. Scores and interactions among the ligands screened through molecular docking, druggability metrics, predictive pharmacokinetics, and toxicological *in silico* tests

Ligand	Score	Interactions with MAO-B
Safinamide	89.57	Leu164, Gln206, Try435, Tyr398, Phe343, Leu171, Cys172, Tyr326, Ile199, Ile316 and FAD600
984	96.35	Ile199, Tyr398, tyr435, Cys172, Leu171, Phe168, Trp119, Leu164 and FAD600
627	93.08	Ile316, Pro104, Ile199, Leu171, Phe343, Tyr398, Gln206, Tyr435, Tyr188, Cys172 and FAD600
775	90.73	Ile316, Ile199, Ile198, Cys172, Gly434, Tyr435, Leu171, Tyr326, Pro102 and FAD600
596	89.82	Leu164, Pro104, Ile199, Ile316, Tyr326, Ile198, Leu171, Cys172, Tyr188, Tyr398, Tyr435, Gly434, Gln206, FAD600
939	89.07	Tyr60, Phe343, Tyr398, Tyr435, Cys172, Ile199, Ile316, Tyr326, Leu171, Ile198, Gln206 and FAD600
412	88.77	Ile316, Leu164, Pro104, Ile199, Trp119, Ile198, Cys172, Tyr398, Tyr435, Gly434, Phe343, Leu171, Tyr326, FAD600
309	88.1	Phe343, Tyr398, Tyr434, Cys172, Leu171, Ile198, Tyr326, Ile199, Ile316, Trp119 and Leu164
903	88.09	Ile316, Tyr326, Gln206, Ile198, Tyr435, Tyr398, Ile199, Leu171 and FAD600
325	79.56	Gly434, Cys172, Ile316, Ile199, Phe168, Leu164, Tyr326, Leu171, Tyr398, Try435, FAD600

deactivating the enzyme.¹⁰⁴ Drugs that work through this mechanism, such as rasagiline and selegiline, can only be given once daily to prevent cumulative inhibition surpassing 90% in the brain. Additionally, this impact can be reversed only by the synthesis of new enzymes.¹⁰⁵

To summarize, the molecular docking results demonstrate three key findings: (i) agreement with the crystallographic data of safinamide co-crystallized with MAO-B; (ii) interactions found in the ligands under analysis correspond to residues considered essential for selective enzymatic inhibition; and (iii) the intermolecular interactions observed with the FAD residue imply a reversible inhibition mechanism.

In addition, a methodological aspect of this work must be considered. Water molecules were removed in the docking analysis using the GOLD software, and according to Gaweska and Fitzpatrick,¹ Lys296 in MAO-B interacts with a water molecule that also binds to N5 of the flavin cofactor, influencing the spatial orientation of the amino acids that make up the aromatic cage of MAO-B (Tyr398 and Tyr435), and consequently in the spatial orientation concerning the enzyme's substrates and ligands.

Similarly, Boppana *et al.*⁵⁰ carried out molecular docking analyses in the GLIDE program, followed by refinement via sampling using Monte Carlo mathematical modeling, and observed in 70 MAO-B inhibitors interactions with the amino acids Tyr 60, pro102, Leu 171, Ile 198, Ile 199, Gln 206, Ile 316, Tyr 326, Phe 343, Tyr 398, and Tyr 435, where the compounds classified as having high or moderate inhibitory activity on MAO-B interacted with water or with the amide group of residue Gln 206 through hydrogen interactions.

Therefore, future studies should be conducted to evaluate the influence of water on the ligands analyzed, as reported by LaBute *et al.*¹⁰⁶ concerning the effects of water and interactions mediated by metal centers in molecular docking calculations.

Lastly, computational methods are not exempt from validation by *in vitro* and *in vivo* studies. However, they can reduce costs and times during the early stages of drug discovery by speeding up the conversion of results into qualified results for developing drug candidates, particularly in high-throughput methods that analyze a large number of molecules.¹⁰⁷

Conclusions

This computational study was able to: (i) propose a pharmacophoric model for MAO-B inhibition presenting two aromatic and one hydrogen acceptor regions; (ii) to identify 104 ligands with potential for developing new

MAO-B inhibitors by approaches such as bioisosterism and structural simplification; and (iii) to discover 4 potential selective and reversible MAO-B inhibitors through virtual screening.

According to the results obtained, the substances 1-[[2-(difluoromethoxy)phenyl]methyl]-4-(pyrrolo[3,2-*b*]pyridin-1-ylmethyl)piperidin-4-ol (ligand **775**), 3-[2-(1,3-benzodioxol-5-yl)-2-oxoethyl]-6-bromoquinazolin-4-one (ligand **984**), 6-chloroimidazo[1,2-*a*]pyridin-2-yl)-[4-(2-pyrazol-1-ylethyl)piperidin-1-yl]methanone (ligand **596**), and (2-phenylimidazo[1,2-*a*]pyridin-6-yl)-[(2*R*)-2-pyridin-2-ylpyrrolidin-1-yl]methanone (ligand **627**) present appropriate physicochemical properties for the development of pharmaceutical formulations for oral use, they did not generate toxicity alerts, and present suitable pharmacokinetic features.

As a result, it is anticipated that due to comparison with data from known MAO-B inhibitors in the literature, these compounds present potential as drug leads or candidate to treat central nervous system disorders related to MAO-B higher activity.

Acknowledgments

Acknowledgments are made to the Coordination for the Improvement of Higher Education Personnel (CAPES) and the Postgraduate Program in Pharmaceutical Innovation at the Federal University of Amapá.

Author Contributions

All the authors contributed to different roles for the development of this work. A.L.P.C. conducted the investigation, data curation, formal analysis, project administration and wrote the original draft. H.B.L., A.C.J.S., G.S.O., M.P.B. and C.H.T.P.S. provided support with computing resources, review and editing. L.I.S.H.-M. conceptualized, structured the methodology, provided support with computing resources and funding acquisition, validation, visualization, reviewing, project administration and supervision.

References

1. Gaweska, H.; Fitzpatrick, P. F.; *Biomol. Concepts* **2011**, *2*, 365. [Crossref]
2. Ramsay, R. R.; *Prog. Neuro-Psychopharmacol. Biol. Psychiatry* **2016**, *69*, 81. [Crossref]
3. Youdim, M. B. H.; Edmondson, D.; Tipton, K. F.; *Nat. Rev. Neurosci.* **2006**, *7*, 295. [Crossref]
4. Narayanaswami, V.; Drake, L. R.; Brooks, A. F.; Meyer, J. H.; Houle, S.; Kilbourn, M. R.; Scott, P. J. H.; Vasdev, N.; *ACS Chem. Neurosci.* **2019**, *10*, 1867. [Crossref]

5. Moriguchi, S.; Wilson, A. A.; Miler, L.; Rusjan, P. M.; Vasdev, N.; Kish, S. J.; Rajkowska, G.; Wang, J.; Bagby, M.; Mizrahi, R.; Varughese, B.; Houle, S.; Meyer, J. H.; *JAMA Psychiatry* **2019**, *76*, 634. [Crossref]
6. Jones, D. N.; Raghanti, M. A.; *J. Chem. Neuroanat.* **2021**, *114*, 101957. [Crossref]
7. Nam, M. H.; Sa, M.; Ju, Y. H.; Park, M. G.; Lee, C. J.; *Int. J. Mol. Sci.* **2022**, *23*, 4453. [Crossref]
8. Carradori, S.; Secci, D.; Petzer, J.; *Expert Opin. Ther. Pat.* **2018**, *28*, 211. [Crossref]
9. Steinmetz, K. L.; Spack, E. G.; *BMC Neurol.* **2009**, *9*, S2. [Crossref]
10. Lombardino, J. G.; Lowe III, J. A.; *Nat. Rev. Drug Discovery* **2004**, *3*, 853. [Crossref]
11. Lin, X.; Li, X.; Lin, X.; *Molecules* **2020**, *25*, 1375. [Crossref]
12. Schneidman-Duhovny, D.; Dror, O.; Inbar, Y.; Nussinov, R.; Wolfson, H.; *J. Nucleic Acids Res.* **2008**, *36*, W223. [Crossref]
13. Binding Database Home, <https://www.bindingdb.org>, accessed in September 2024.
14. Koes, D. R.; Camacho, C. J.; *Nucleic Acids Res.* **2012**, *40*, W409. [Crossref]
15. OMEGA, 5.1.0.0.; OpenEye, Cadence Molecular Sciences, United States. [Link] accessed in September 2024
16. ROCS, 3.4; OpenEye Scientific Software, United States, 2022. [Link] accessed in September 2024
17. Hawkins, P. C. D.; Skillman, A. G.; Nicholls, A.; *J. Med. Chem.* **2007**, *50*, 74. [Crossref]
18. EON, 3.1; OpenEye Scientific Software, United States, 2023. [Link] accessed in September 2024
19. Muchmore, S. W.; Souers, A. J.; Akritopoulou-Zanze, I.; *Chem. Biol. Drug Des.* **2006**, *67*, 174. [Crossref]
20. GOLD, 2023.1; Cambioso Risso, United Kingdom, 2023. [Link] accessed in September 2024
21. Verdonk, M. L.; Cole, J. C.; Hartshorn, M. J.; Murray, C. W.; Taylor, R. D.; *Proteins: Struct., Funct., Bioinf.* **2003**, *52*, 609. [Crossref]
22. QikProp, 6.9; Schrödinger, LLC, United States, 2023. [Link] accessed in September 2024
23. Laoui, A.; Polyakov, V. R.; *J. Comput. Chem.* **2011**, *32*, 1944. [Crossref]
24. DEREK Nexus, 6.2; Lhasa Limited, United Kingdom, 2022. [Link] accessed in September 2024
25. Ahuja, V.; Krishnappa, M.; *Toxicol. Lett.* **2022**, *368*, S286. [Crossref]
26. SwissADME, www.swissadme.ch/index.php, accessed in January 2024.
27. Daina, A.; Michielin, O.; Zoete, V.; *Sci. Rep.* **2017**, *7*, 42717. [Crossref]
28. Mvondo, J. G. M.; Matondo, A.; Mawete, D. T.; Bambi, S.-M. N.; Mbala, B. M.; Lohohola, P. O.; *Int. J. Trop. Dis. Health* **2021**, *42*, 1. [Crossref]
29. Carradori, S.; D'Ascenzio, M.; Chimenti, P.; Secci, D.; Bolasco, A.; *Mol. Diversity* **2014**, *18*, 219. [Crossref]
30. Baweja, G. S.; Gupta, S.; Kumar, B.; Patel, P.; Asati, V.; *Mol. Diversity* **2023**, *28*, 1823. [Crossref]
31. Gilson, M. K.; Liu, T.; Baitaluk, M.; Nicola, G.; Hwang, L.; Chong, J.; *Nucleic Acids Res.* **2016**, *44*, 1045. [Crossref]
32. Wassermann, A.; Bajorath, J.; *Expert Opin. Drug Discovery* **2011**, *6*, 683. [Crossref]
33. Wang, W.; Song, K.; Li, L.; Chen, L.; *Curr. Top. Med. Chem.* **2018**, *18*, 998. [Crossref]
34. Hu, B.; Zhu, X.; Monroe, L.; Bures, M.; Kihara, D.; *Int. J. Mol. Sci.* **2014**, *15*, 15122. [Crossref]
35. Verdonk, M. L.; Berdini, V.; Hartshorn, M. J.; Mooij, W. T. M.; Murray, C. W.; Taylor, R. D.; Watson, P.; *J. Chem. Inf. Comput. Sci.* **2004**, *44*, 793. [Crossref]
36. Kramer, J. A.; Sagartz, J. E.; Morris, D. L.; *Nat. Rev. Drug Discovery* **2007**, *6*, 636. [Crossref]
37. Bouchet, S.; Molimard, M.; *Therapies* **2022**, *77*, 157. [Crossref]
38. Batchelor, H. K.; Marriott, J. F.; *Br. J. Clin. Pharmacol.* **2015**, *79*, 395. [Crossref]
39. Mangoni, A. A.; Jackson, S. H. D.; *Br. J. Clin. Pharmacol.* **2004**, *57*, 6. [Crossref]
40. Vargason, A. M.; Anselmo, A. C.; Mitragotri, S.; *Nat. Biomed. Eng.* **2021**, *5*, 951. [Crossref]
41. Adepu, S.; Ramakrishna, S.; *Molecules* **2021**, *26*, 5905. [Crossref]
42. Marchant, C. A.; Briggs, K. A.; Long, A.; *Toxicol. Mech. Methods* **2008**, *18*, 177. [Crossref]
43. Holdgate, G. A.; Meek, T. D.; Grimley, R. L.; *Nat. Rev. Drug Discovery* **2018**, *17*, 115. [Crossref]
44. Salman, M. M.; AL-Obaidi, Z.; Kitchen, P.; Loreto, A.; Bill, R. M.; Wade-Martins, R.; *Int. J. Mol. Sci.* **2021**, *22*, 4688. [Crossref]
45. Camarena, B.; Fresán, A.; Aguilar, A.; Escamilla, R.; Saracco, R.; Palacaios, J.; Nicolini, H.; *ISRN Psychiatry* **2012**, ID 852949. [Crossref]
46. Liu, Y.; Wang, Z.; Zhang, B.; *Ann. Saudi Med.* **2014**, *34*, 12. [Crossref]
47. Löhle, M.; Mangone, G.; Hermann, W.; Hausbrand, D.; Wolz, M.; Mende, J.; Reichmann, H.; Hermann, A.; Corvel, J.-C.; Storch, A.; *Parkinson's Dis.* **2022**, *1*, 2022. [Crossref]
48. Zapała, B.; Stefura, T.; Piwowar, M.; Czekalska, S.; Zawada, M.; Hadasik, M.; Solnica, B.; Rudzińska-Bar, M.; *J. Mol. Neurosci.* **2022**, *72*, 812. [Crossref]
49. Gritsch, S.; Guccione, S.; Hoffmann, R.; Cambria, A.; Raciti, G.; Langer, T.; *J. Enzyme Inhib. Med. Chem.* **2001**, *16*, 199. [Crossref]
50. Boppana, K.; Dubey, P. K.; Jagarlapudi, S. A. R. P.; Vadivelan, S.; Rambabu, G.; *Eur. J. Med. Chem.* **2009**, *44*, 3584. [Crossref]

51. de Souza, L. R.; Picanço, R. M.; Pinheiro, A. A.; da Silva, K. R.; Taft, C. A.; da Silva, C. H. T. P.; dos Santos, C. B. R.; Hage-Melim, L. I. S.; *Curr. Org. Chem.* **2016**, *6*, 40. [Crossref]
52. Perola, E.; Charifson, P. S.; *J. Med. Chem.* **2004**, *47*, 2499. [Crossref]
53. Boström, J.; Grant, J. A.; Fjellström, O.; Thelin, A.; Gustafsson, D.; *J. Med. Chem.* **2013**, *53*, 3273. [Crossref]
54. Venhorst, J.; Núñez, S.; Terpstra, J. W.; Kruse, C.; *J. Med. Chem.* **2008**, *51*, 3222. [Crossref]
55. Crisan, L.; Istrate, D.; Bora, A.; Pacureanu, L.; *Mol Diversity* **2021**, *25*, 1775. [Crossref]
56. Hagenow, J.; Hagenow, S.; Grau, K.; Khanfar, M.; Hefke, L.; Proschak, E.; Stark, H.; *Drug Des., Dev. Ther.* **2020**, *2020*, 371. [Crossref]
57. Mateeve, E.; Valkova, I.; Angelov, B.; Georgieva, M.; Zlatkov, A.; *Int. J. Pharm. Sci.* **2022**, *13*, 1099. [Crossref]
58. Binda, C.; Aldeco, M.; Mattevi, A.; Edmondson, D. E.; *J. Med. Chem.* **2011**, *54*, 909. [Crossref]
59. Smith, G. R.; Sternberg, M. J. E.; *Curr. Opin. Struct. Biol.* **2002**, *12*, 28. [Crossref]
60. Korb, O.; Stütze, T.; Exner, T. E.; *J. Chem. Inf. Model.* **2009**, *49*, 84. [Crossref]
61. Spundzhi, F.; Dzimbova, T.; Pencheva, N.; Milanov, P.; *Bulg. Chem. Commun.* **2017**, *49*, 23. [Link] accessed in September 2024
62. Li, J.; Fun, A.; Zhang, L.; *Interdiscip. Sci.: Comput. Life Sci.* **2019**, *11*, 320. [Crossref]
63. Amoroso, N.; Gambacorta, N.; Mastrolorito, F.; Togo, M. V.; Trisciuzzi, D.; Monaco, A.; Altomare, C. D.; Ciriaco, F.; Nicolotti, O.; *Sci. Rep.* **2023**, *13*, 21335. [Crossref]
64. Vogt, M.; *Expert Opin Drug Discov.* **2022**, *3*, 297. [Crossref]
65. Barnham, K. J.; Masters, C. L.; Bush, A. I.; *Nat. Rev. Drug Discovery* **2004**, *3*, 205. [Crossref]
66. O'Brien, Z.; Moghddam, M. F.; *Curr. Med. Chem.* **2017**, *14*, 3159. [Crossref]
67. Morofuji, Y.; Nakagawa, S.; *Curr. Pharm. Des.* **2020**, *26*, 1466. [Crossref]
68. Meanwell, N. A.; *Burger's Medicinal Chemistry and Drug Discovery* **2021**, *1*. [Crossref]
69. Wang, S.; Dong, G.; Sheng, C.; *Acta Pharm. Sin. B* **2019**, *9*, 880. [Crossref]
70. Park, Y.-C.; Lee, S.; Cho, M.-H.; *Toxicol. Res.* **2014**, *30*, 179. [Crossref]
71. Tennekes, H. A.; Sánchez-Bayo, F.; *Toxicology* **2013**, *309*, 39. [Crossref]
72. Borgert, C. J.; Fuentes, C.; Burgoon, L. D.; *Arch. Toxicol.* **2021**, *95*, 3651. [Crossref]
73. Barouki, R.; Audouze, K.; Becker, C.; Blaha, L.; Coumoul, X.; Karakitsios, S.; Klanova, J.; Miller, G. W.; Price, E.; Saragiannis, D.; *Toxicol. Sci.* **2022**, *186*, 1. [Crossref]
74. Knudsen, T. B.; Spencer, R. M.; Pierro, J. D.; Baker, N. C.; *Curr. Opin. Toxicol.* **2020**, *23-24*, 119. [Crossref]
75. Pognan, F.; Beilmann, M.; Boonen, H. C. M.; Czich, A.; Dear, G.; Hewitt, P.; Mow, T.; Oinonen, T.; Roth, A.; Steger-Hartmann, Valentin, J.-P.; Van Goethem, F.; Weaver, R. J.; Newham, P.; *Nat. Rev. Drug Discovery* **2023**, *22*, 317. [Crossref]
76. Raunio, H.; *Front. Pharmacol.* **2021**, *2*, 33. [Crossref]
77. Gampe, N.; Dávid, D. N.; Takács-Novák, K.; Backlund, A.; Béni, S.; *Plos One* **2022**, *17*, e0265639. [Crossref]
78. Jost, W. H.; *J. Neural Transmission* **2022**, *129*, 723. [Crossref]
79. Hemmerich, J.; Ecker, G. F.; *Wiley Interdiscip. Rev.: Comput. Mol. Sci.* **2020**, *10*, e1475. [Crossref]
80. Deiab, G. I. A.; Saadah, L. M.; Basheti, I. A.; *Braz. J. Pharm. Sci.* **2022**, *58*, e21070. [Crossref]
81. Ioakimidis, L.; Thoukydidis, L.; Mirza, A.; Maeem, S.; Reynisson, J.; *Mol. Inf.* **2008**, *27*, 445. [Crossref]
82. Hage-Melim, L. I. S.; Federico, L. B.; Oliveira, N. K. S.; Francisco, V. C. C.; Correia, L. C.; Lima, H. B.; Gomes, S. Q.; Barcelos, M. P.; Francischini, I. A. G.; Silva, C. H. T. P.; *Life Sci.* **2020**, *256*, 117963. [Crossref]
83. Benet, L. Z.; Hosey, C. M.; Ursu, O.; Oprea, T. I.; *Adv. Drug Delivery Rev.* **2016**, *101*, 89. [Crossref]
84. Yim, D.-S.; Choi, S.; *Transl. Clin. Pharmacol.* **2020**, *28*, 169. [Crossref]
85. Flores-Holguín, N.; Frau, J.; Glossman-Mitnik, D.; *ChemistryOpen* **2021**, *10*, 1142. [Crossref]
86. Hosen, S.; Dash, R.; Khatun, M.; Akter, R.; Bhuiyan, H. R.; Karim, R.; Mouri, N. J.; Ahamed, F.; Islam, K. S.; Afrin, S.; *J. Appl. Pharm. Sci.* **2017**, 120. [Crossref]
87. Urquhart, B.; Kim, R. B.; *Eur. J. Clin. Pharmacol.* **2009**, *65*, 1063. [Crossref]
88. Stieger, B.; Gao, B.; *Clin. Pharmacokinet.* **2015**, *54*, 225. [Crossref]
89. Upton, R. N.; *Clin. Exp. Pharmacol. Physiol.* **2007**, *34*, 695. [Crossref]
90. Srinivas, N.; Maffuid, K.; Kashuba, A. D. M.; *Clin. Pharmacokinet.* **2018**, *57*, 1059. [Crossref]
91. Ntie-Kang, F.; Lifongo, L. L.; Mbah, J. A.; Owono, L. C. O.; Megnassan, E.; Mbaze, L. M.; Judson, P. N.; Sippl, W.; Efange, S. M. N.; *In Silico Pharmacol.* **2013**, *1*, 12. [Crossref]
92. Fatima, S.; Gupta, P.; Sharma, S.; Sharma, A.; Agarwal, S. M.; *Future Med. Chem.* **2019**, *12*, 69. [Crossref]
93. Zhao, M.; Ma, J.; Li, M.; Zhang, y.; Jiang, B.; Zhao, X.; Huai, C.; Shen, L.; Zhang, N.; He, L.; Qin, S.; *Int. J. Mol. Sci.* **2021**, *22*, 12808. [Crossref]
94. Tracy, T. S.; Vankataramanan, R.; Glover, D. D.; Caritis, S. N.; *Am. J. Obstet. Gynecol.* **2005**, *192*, 633. [Crossref]
95. Lynch, T.; Price, A.; *Am. Fam. Physician* **2007**, *76*, 391. [Crossref]

96. Levêque, D.; Lemachatti, J.; Nivoix, Y.; Coliat, P.; Santucci, R.; Ubeaud-Séquier, G.; Beretz, L.; Vinzio, S.; *La Revue de Médecine Interne*. **2010**, *31*, 170. [Crossref]
97. Binda, C.; Wang, J.; Pisani, L.; Caccia, C.; Carotti, A.; Salvati, P.; Edmondson, D. E.; Mattevi, A.; *J. Med. Chem.* **2007**, *50*, 5848. [Crossref]
98. Harkcom, W. T.; Bevan, D. R.; *Biochem. Biophys. Res. Commun.* **2007**, *360*, 401. [Crossref]
99. Mateev, E.; Georgieva, M.; Mateeva, A.; Zlatkov, A.; Ahmad, S.; Raza, K.; Azevedo, V.; Barh, D.; *Molecules* **2023**, *28*, 4814. [Crossref]
100. Mettai, M.; Daoudi, I.; Mesli, F.; Kenouche, S.; Melkemi, N.; Kherachi, R.; Belkadi, A.; *Molecules* **2023**, *11*, 3. [Crossref]
101. Reyes-Parada, M.; Fierro, A.; Iturriaga-Vasquez, P.; Cassels, B.; *Curr. Enzyme Inhib.* **2005**, *1*, 85. [Crossref]
102. Shetnev, A. A.; Efimova, J. A.; Korsakov, M. K.; Petzer, A.; Petzer, J. P.; *Molecules* **2024**, *2024*, M1787. [Crossref]
103. Bissantz, C.; Kuhn, B.; Stahl, M.; *J. Med. Chem.* **2010**, *53*, 5061. [Crossref]
104. Tandarić, T.; Vianello, R.; *ACS Chem. Neurosci.* **2019**, *10*, 3532. [Crossref]
105. Finberg, J. P. M.; Rabey, J. M.; *Front. Pharmacol.* **2016**, *7*, 340. [Crossref]
106. Labute, M. X.; Zhang, X.; Lenderman, J.; Bennion, B. J.; Wong, S. E.; Lightstone, F. C.; *PLoS One* **2014**, *9*, e106298. [Crossref]
107. Kassel, D. B.; *Curr. Opin. Chem. Biol.* **2004**, *8*, 339. [Crossref]

Submitted: June 1, 2024

Published online: September 30, 2024